Nakamura *et al.*
Progress in Earth and Planetary Science (2023) 10:45
https://doi.org/10.1186/s40645-023-00579-7

Progress in Earth and Planetary Science

RESEARCH ARTICLE

Open Access

Incoming plate structure at the Japan Trench subduction zone revealed in densely spaced reflection seismic profiles

Yasuyuki Nakamura[1*], Shuichi Kodaira[1], Gou Fujie[1], Mikiya Yamashita[1,2], Koichiro Obana[1] and Seiichi Miura[1]

Abstract

The structure of the incoming plate is an important element that is often considered to be related to the occurrence of great earthquakes in subduction zones. In the Japan Trench, where the 2011 Tohoku earthquake occurred, we collected seismic profiles along survey lines separated by 2–8 km to examine the structural characteristics of the incoming Pacific plate in detail. The average thickness of the incoming sediments was < 500 m along most of the Japan Trench, and it was < 300 m at ~ 38° N, where the large shallow megathrust slip occurred during the 2011 Tohoku earthquake. We mapped bending-related normal faults, including their dip direction and amount of throw. The numbers of eastward (oceanward) and westward (trenchward) dipping normal faults were generally comparable in the Japan Trench. Eastward dipping normal faults were dominant in the northern and southern parts of the Japan Trench, whereas westward dipping normal faults were more numerous in the central part. Graben-fill sediments deposited at the landward edge of the graben were bounded by eastward dipping normal faults. Trench-fill sediments were also observed along the trench axis. The sediment fills locally increased the thickness of the input sediments where they were deposited. The along-axis variation in input sediment and sediment fill distribution, and the variations in normal fault dip direction between the central and other parts of the Japan Trench may correspond to different slip styles along the plate boundary.

Keywords Japan Trench, Incoming structure, Sediment thickness, Normal faults, Subduction zone earthquake

1 Introduction

The Tohoku earthquake occurred in March 2011 in the Japan Trench subduction zone. Numerous studies have been conducted to understand this one of the greatest earthquakes. Various rupture models were obtained using seismological, geodetic, and tsunami datasets (e.g., Ide et al. 2011; Iinuma et al. 2012; Satake et al. 2013). Most of them suggested that large slip occurred in the shallowest megathrust near the trench axis and large slip area is limited to relatively small area in the central part of the Japan Trench (Lay 2018). The analysis from the fault zone samples obtained from the drilling into the shallowest megathrust (Chester et al. 2013) suggested that the large shallow slip was facilitated by the smectite with very low frictional coefficients in the fault zone and thermal pressurization (Ujiie et al. 2013).

Recently, slow earthquakes have been observed in the subduction zones (e.g., Ito and Obara 2006; Todd and Schwartz 2016; Dragert et al. 2004). These slow earthquakes, which are the fault slip phenomenon different from the "normal" earthquakes, are thought to be important to understand the megathrust fault slip in the subduction zones. In the Japan Trench, various types of slow

*Correspondence:
Yasuyuki Nakamura
yasu@jamstec.go.jp
Full list of author information is available at the end of the article

earthquakes (tremor, low-frequency earthquake (LFE), very low-frequency earthquake (VLFE), slow slip event (SSE)) have been reported in recent years (e.g., Nishikawa et al. 2019). A M7 slow slip event preceded the Tohoku earthquake within the rupture zone of the Tohoku earthquake (e.g., Ito et al. 2013). As pointed out by Nishikawa et al. (2023), the source region of the 2011 Tohoku earthquake and the "seismic" slow earthquakes (tremors and VLFEs) are complimentary distributed in the along-strike direction on a scale of hundreds of kilometers (Nishikawa et al. 2019; Baba et al. 2020). It was also pointed out that the distribution of fast and slow earthquakes is complex in both along-strike and along-dip directions on a scale of tens of kilometers (Nishikawa et al 2019; Nishimura 2021; Obana et al. 2021).

The variation of the slip styles mentioned above should be linked to the structure in the subduction zone. Since the 1980s, many structural studies have been carried out in the Japan Trench subduction zone, showing the subduction of the horst–graben structure formed by bending-related normal faults (e.g., von Huene and Culotta 1989), the development of the bending-related normal faults from outer rise to beneath the subduction zone (Tsuru et al. 2000), wedge-shaped frontal prism beneath the lowermost landward slope with low p-wave velocity (e.g., Tsuru et al. 2000; Takahashi et al. 2004). After the 2011 Tohoku earthquake, several studies were conducted to elucidate the structural characteristics in its rupture zone. The shallowest part of the subduction zone with the large coseismic slip indicates the fold-and-thrust deformation structures in the vicinity of the trench axis (Kodaira et al. 2012; Nakamura et al. 2013, 2020), but such deformation structure was not observed in the southern part of the Japan Trench where large coseismic slip did not occur (Qin et al. 2022). The frontal prism beneath the lowermost landward slope and the backstop interface landward of the prism are imaged in the northern part, whereas the channel-like structure above the subducting oceanic plate is imaged in the southern part of the Japan Trench (Tsuru et al. 2002). Kodaira et al. (2017) demonstrated that the frontal prism is also imaged in the rupture zone of the Tohoku earthquake in the central part of the Japan Trench. Tomographic studies showed that the rupture of the Tohoku earthquake was initiated at the boundary between high- and low-velocity areas in the megathrust zone (Zhao et al. 2011; Hua et al. 2020). Bassett et al. (2016) showed that the residual bathymetric and gravity anomalies observed in the forearc of the southern Japan Trench correspond to the southern extent of the 2011 Tohoku earthquake rupture zone.

The structural variation in the subduction zone should be related to the structure of the subduction inputs. Then, the characteristics of the input structure in the subduction zone have been regarded as one of the key factors to understand the megathrust slip behaviors. Subducted seamounts have been thought to act as asperities (e.g., Cloos 1992). Recent studies suggested that the seamount subducts aseismically (e.g., Mochizuki et al. 2008). The thick incoming sediments are thought to be favorable conditions for great subduction zone earthquakes (e.g., Heuret et al. 2012). In the Japan Trench, the oceanic Pacific plate shows well-developed horst-and-graben related to the bending-related normal faults. The normal fault distribution has variations along the trench from north to south, and it is complicated in the central Japan Trench (Nakanishi 2011). The P-wave velocity structures suggest that the crust and the uppermost mantle in the incoming Pacific plate are hydrated near the trench due to the bending-related normal faults (e.g., Fujie et al. 2016, 2018). Several petit-spot sites were reported on the incoming Pacific plate, and one of them is located near the northern end of the large slip zone of the Tohoku earthquake (Hirano et al. 2006). Fujie et al. (2020) suggested that the petit-spot activity altered the incoming sediments, which prevented the northward propagation of megathrust shallow slip during the Tohoku earthquake. Boston et al. (2014) investigated the incoming plate structure in the central part of the Japan Trench at 37.5°–39° N and interpreted the bending-related normal faults and thickness of the sediments with the depth-migrated seismic profiles. The thickness of the sediments varies between 0 and 600 m and is generally increased toward the trench in their study area. Throws of bending-related normal faults are more in the north than south in the survey area. They proposed that seaward propagation of the shallow-most decollement is related to the normal faults including those densely developed within the sediment column. Qin et al. (2022) interpreted the seismic profiles in the southern part of the Japan Trench between 36° and 37.5° N, mostly outside the rupture zone of the 2011 Tohoku earthquake and divided the study area into 4 segments based on structural variations. They indicated that their northern segment within the 2011 rupture zone has thinner incoming sediments and a dense distribution of the horst-and-graben features. They inferred that the roughness of the incoming plate basement affects on the physical properties in the plate boundary and the hanging wall, which causes the variation of the seismic behavior in the subduction zone. To the north, Tanioka et al. (1996) argued that the bathymetric feature on the incoming plate in the source region of 1896 Meiji Sanriku tsunami earthquake, which partially overlapped with the 2011 Tohoku earthquake source region, is rough, and it contributed to the slow rupture process during the Meiji Sanriku earthquake.

Thus, the incoming structure in the Japan Trench partly indicates the correspondence to the megathrust slip behaviors; however, the detailed linkage between the incoming structure and the complicated distribution of the various types of the megathrust slips, including the slow earthquakes, is still unclear. The detailed subsurface structure has not been studied in the northern Japan Trench, where the tsunami earthquake occurred and slow earthquakes have been recently reported. In this paper, we use the seismic profiles densely acquired in the vicinity of the Japan Trench which mostly cover the entire extent of the Japan Trench, to map the structural features of the incoming plate. The along-axis variation of the incoming structure is investigated in detail along the entire Japan Trench. We map the distribution of the normal faults and the thickness of the incoming sediments along with the distribution of sediment fills. We then infer the correspondence between these structural characteristics to the megathrust slip phenomenon.

2 Data and methods

The seismic dataset used in this study was collected during cruises KR13-06 and KR13-11 of R/V *Kairei* in 2013, KY14-E02 and KY15-14 of R/V *Kaiyo* in 2014 and 2015, and YK16-17 and YK17-22 of R/V *Yokosuka* in 2016 and 2017 (Fig. 1). A digital streamer cable with 168–192 channel hydrophones attached at 6.25 m intervals and towed at 6 m depth recorded seismic signals from an array of airguns (6.23 L) towed at 5 m depth. The data were sampled at 1 ms intervals, and airguns were fired every 37.5 m (or 50 m along some lines) with 13.8 MPa of air pressure. We used conventional procedures, including CMP sorting, normal move out, stacking, and post stack time migration (Nakamura et al. 2013), to obtain the best time-migrated images from the recorded data. We applied an F-K migration with constant velocity model (1525 m/s) because the length of the cable was too short to determine the velocities. In this study, we focused on the structure of the incoming plate east of the Japan trench axis. The time-migrated seismic profile along each of 120 seismic lines was interpreted to map geological structures, including normal faults, sediments, and the basaltic basement of the incoming Pacific plate.

We interpreted normal faults that clearly offset the top of chert layer or oceanic crust with strong reflections (see Sect. 3.1). The vertical fault throw was measured from the two-way travel time (TWT) difference between the shallowest strong reflections on either side of the normal fault.

3 Results

3.1 Seismic profiles

Figure 2 shows a typical seismic profile of the incoming Pacific plate east of the Japan Trench. We interpreted seismic profiles with reference to the results from DSDP Site 436 (Shipboard Scientific Party 1980) on the outer rise in the northern Japan Trench. The top seismic unit, which is characterized by relatively weak continuous or semi-continuous reflections generally sub-parallel to the seafloor, was interpreted to consist mainly of soft hemipelagic sediments. The next underlying unit is characterized by strong reflections and was interpreted to include hard sediments such as chert. The lowest unit is the acoustic basement, interpreted as igneous oceanic crust. These units correspond to Seismic Unit 2 (SU2), SU3, and SU4, respectively, of Nakamura et al. (2013, 2020). (Note that another seismic unit, SU1, was identified within and landward of the trench axis, and was interpreted as frontal prism sediments.) Clearly imaged normal faults caused by bending of the subducting plate (e.g., Tsuru et al. 2000) cut SU2–4. In some grabens and other locations along the trench axis, wedge-shaped sediment-fill packages overlie the landward dipping incoming sediments or even the seaward tip of the frontal prism sediments (SU1) (e.g., "graben fill" in Fig. 2). The facies of the sediment-fill are parallel onlap fill, and chaotic or reflection-free fills. The onlap fills are bounded by angular unconformities from underlying landward-tilted sediments. In this study, we defined a sediment fill observed in the trench axis area where the water depth was greatest as the "trench fill," and we defined a sediment fill observed in grabens on the oceanward trench slope as "graben fill."

We mapped the distribution of bending-related normal faults and their throws, and the thickness of the incoming sediments and sediment fills along almost the entire length of the Japan Trench from the Daiichi Kashima

(See figure on next page.)

Fig. 1 Map of the study area and seismic lines. Yellow lines indicate seismic survey lines used in this study. Seismic profiles along the red lines are shown in Figs. 2, 3, 4, 5. Orange dashed lines with arrowheads indicate the three segments inferred in this study. The red star denotes the epicenter of the 2011 Tohoku earthquake. White contours show the slip distribution during the Tohoku earthquake (from Iinuma et al. 2012): Dashed, thin solid, and bold solid lines denote 10 m, 30 m, and 50 m slips, respectively. Green crosses and open circles indicate tremors and very low-frequency earthquakes, respectively (from Nishikawa et al. 2019). The green shaded rectangle denotes the slow slip event in 2011 (Ito et al. 2013). The magenta shaded rectangles indicate the area where chert layers are apparently missing (according to Fujie et al. 2020). Cyan dashed rectangles are the source location of 1933 Showa Sanriku earthquake (Uchida et al. 2016). Gray thick dashed lines show the possible pseudofaults (Nakanishi 2011). Black contours show the bathymetry (interval, 1000 m). Abbreviation: smt, seamount

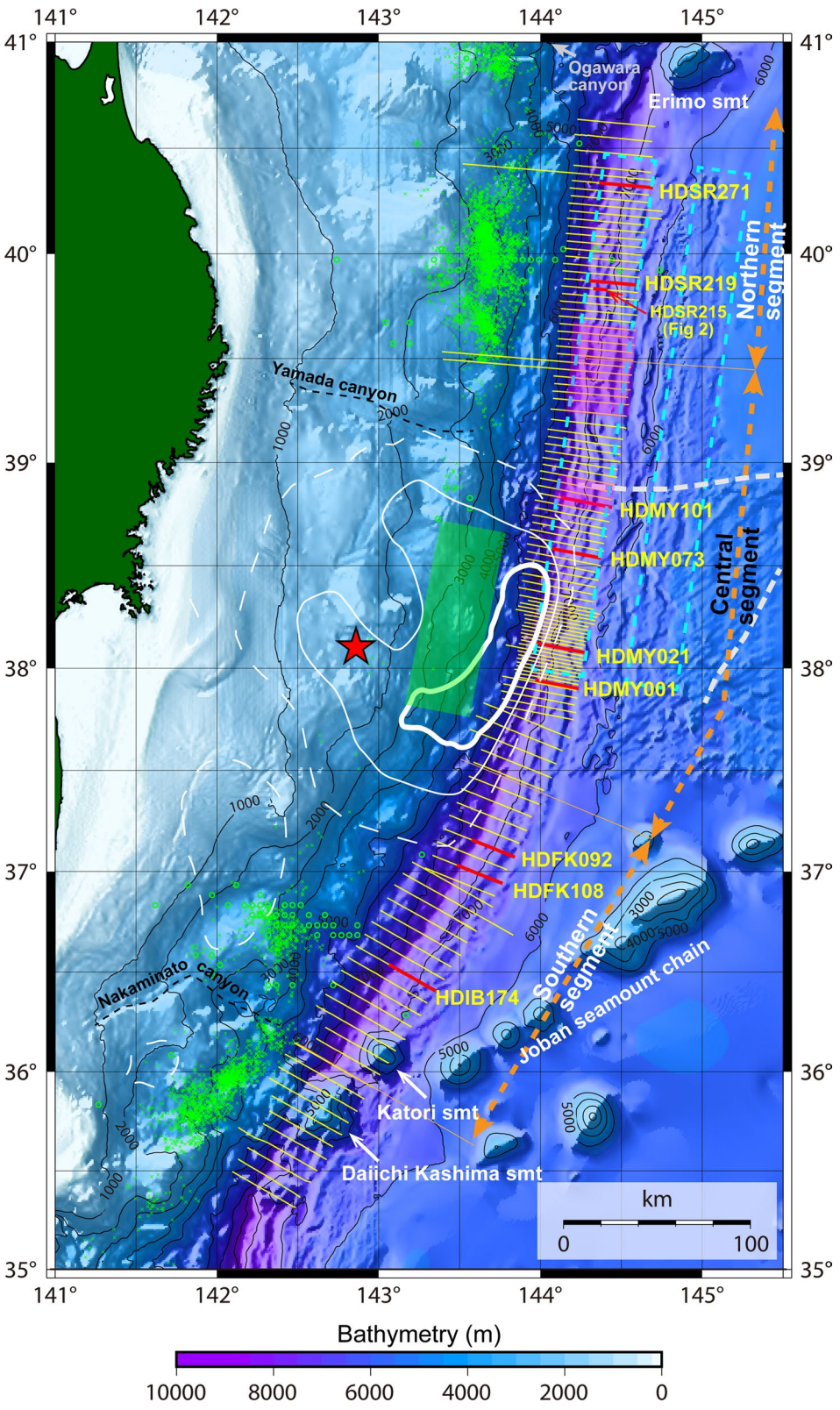

Fig. 1 (See legend on previous page.)

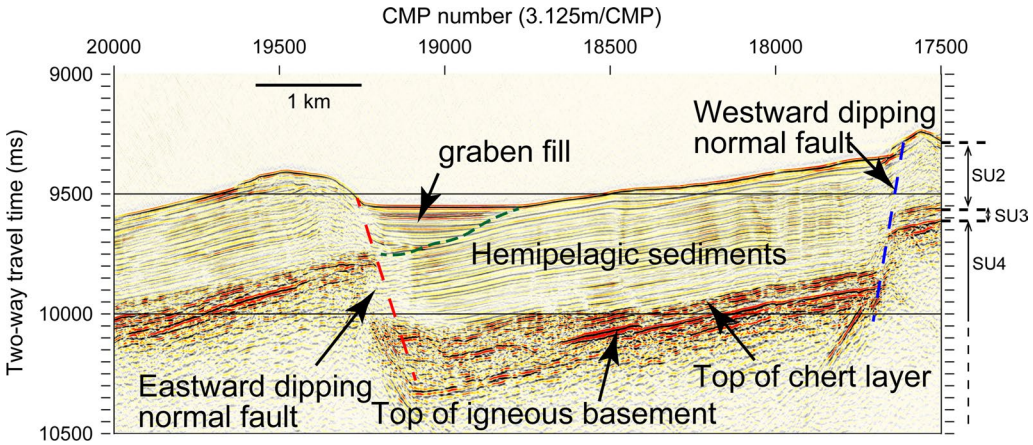

Fig. 2 An example of a typical seismic profile. The location of the profile is shown in Fig. 1. The profile depicts the shallow structure of the incoming Pacific plate in the Japan Trench region. Green dashed line is the bottom of the graben fill

seamount in the south to the Erimo seamount in the north. We divided the Japan Trench along its strike into three segments, northern (north of 39.5° N), central (37.5°–39.5° N), and southern (south of 37.5° N) segments, based on the mapped structural characteristics (See also Fig. 1), which are described and discussed in following sections. Figures 3, 4, 5 demonstrate the selected profiles used in this study, from northern (Fig. 3), central (Fig. 4), and southern (Fig. 5) segments of the Japan Tre nch.

3.2 Normal faults

Normal faults have developed in the outer area of the Japan Trench up to ~ 100 km eastward (oceanward) of the trench (Tsuru et al. 2000). These normal faults were most likely produced by the bending of the incoming plate during its subduction into the trench. The seismic lines used in this study did not cover the entire extent of the outer rise, but the profiles clearly show normal faults up to ~ 20 to 30 km eastward of the trench in the area covered by the seismic lines (Figs. 3, 4, 5). Figure 6 shows the distribution of bending-related normal faults, along with their dip direction and vertical throw where each fault contacts SU3 or SU4 in the footwall. The thickness of the SU3 is variable and could be very thin. The dominant frequency of our seismic data is ~ 50 Hz, which could bring > 20 ms uncertainty in estimating the fault throw where SU3 is not obviously interpreted. The fault distribution generally follows seafloor scarps. The fault throws of ~ 70% of the normal faults are < 200 ms, but throws are larger in some places, especially around 39.5°N where the throws reach > 500 ms.

The distribution of dip directions of normal faults varies along the Japan Trench. We calculated the average number of normal faults with an eastward or westward dip per seismic line over every 0.5° of latitude (Fig. 7a). We also calculated the cumulative throw of normal faults with each dip direction along each line and averaged the cumulative throws per line over every 0.5° (Fig. 7b). We counted all normal faults with > 50 ms of vertical offset. The number of faults and cumulative throws for each line was normalized by the length of each survey line on the incoming plate. The average number and cumulative throws assuming 30 km as the survey lines are shown in Fig. 7a and b. Note, however, that our survey lines covered only the trenchward part of the outer rise region. The average throw of a single fault was also comparable between the two dip directions in most parts of the Japan Trench (Fig. 7c). Although overall the cumulative throw and the number of the normal faults in each dip direction were generally comparable, they showed along-trench variations. The cumulative throw of westward dipping normal faults was relatively larger at 38°–39.5° N, whereas those of eastward dipping normal faults were relatively larger at 39.5°–40.5° N and 36.5°–37.5° N. The normal faults dipping eastward are more numerous at 36.5°–37° N and at 40°–40.5° N, and those dipping westward are more numerous at 38.5°–39° N. The average throw of a normal fault is comparable in each dip direction, except for 37°–37.5° N. We also observed that cumulative throws of the eastward dipping faults are almost constant between 36.5° and 41.0° N; however, those of westward dipping faults indicated variation with their peak at 38.5°–39° N, which causes the variation of dominance in the dip direction.

3.3 Sediment thickness

The sediments on the incoming plate are basically composed of SU2 and SU3. In this study, we regard the SU2 and sediment fills deposited above SU2 as the incoming

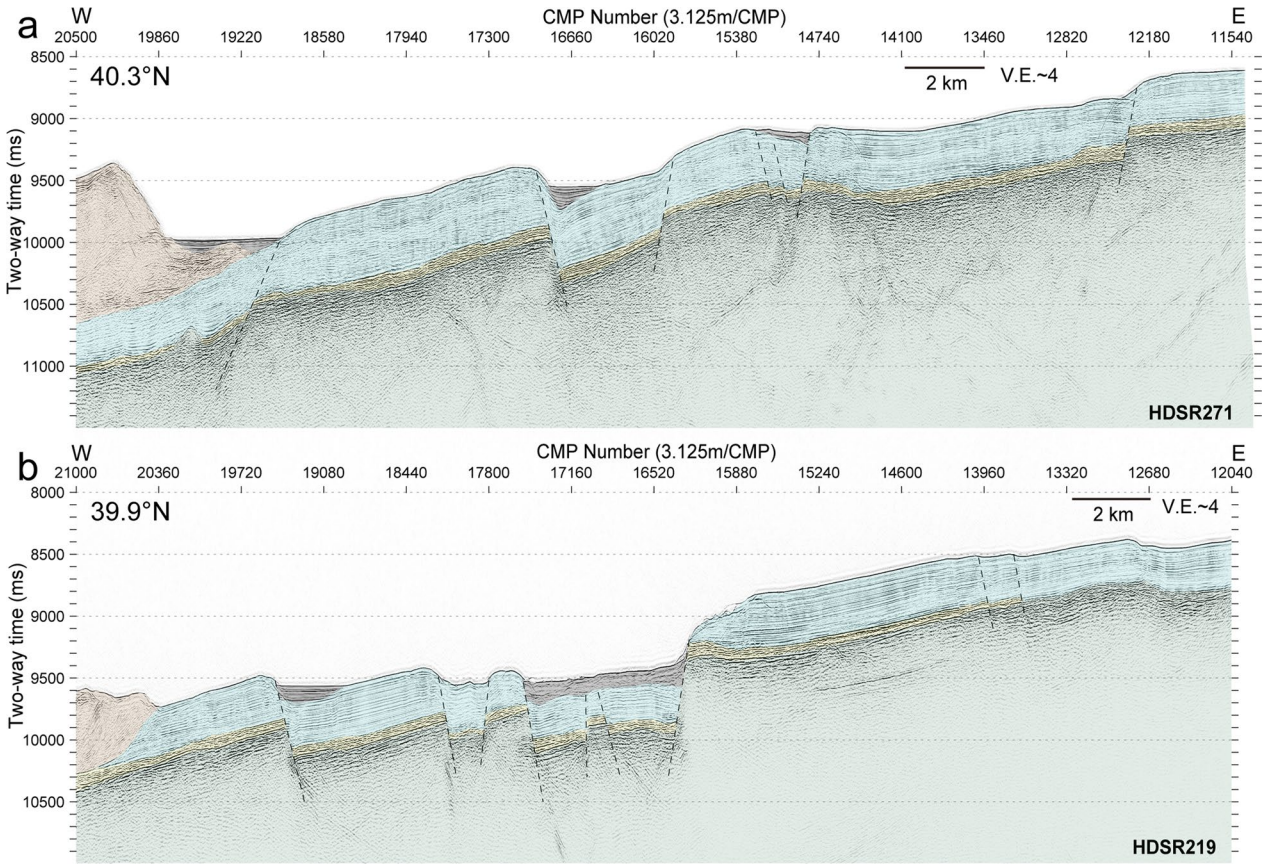

Fig. 3 Selected seismic profiles in the northern part of the Japan Trench. Poststack time-migrated profiles with interpretation are shown. Brown, blue, yellow, and green shadings indicate seismic units SU1, SU2, SU3, and SU4, respectively. Gray shading indicates interpreted sediment fills. Bending-related normal faults are drawn with black dashed lines. The location of each profile is shown in Fig. 1

sediments to map, because the shallowest decollement in the Japan Trench subduction zone is developed above the chert (SU3) (e.g., Kodaira et al. 2012; Chester et al. 2013; Nakamura et al. 2013). Note that the seaward tip of the frontal prism sediments (SU1) is also included at the trench axis in some locations. Thickness of the incoming sediments varied along the trench from 0 to > 600 ms of TWT (Fig. 8). At around 36.5°N, the incoming sediment was thick, with TWT greater than 500 ms (e.g., Line HDIB174; Fig. 5c). In 36.7°–37.3° N, the sediment thickness was ~ 300–400 ms in general, but it became > 600 ms near the trench axis (e.g., Line HDFK092; Fig. 5a). Another thick area was aligned along a graben (e.g., Line HDFK108 around CMP 11000; Fig. 5b, see also Fig. 8). This thickening is due to the trench and graben fills as imaged on the seismic profiles (see also Sect. 3.4). The sediment thickness was relatively constant at about 200–350 ms at 37.3°–38.5° N (e.g., HDMY001, HDMY021; Fig. 4c, d), but the thickness was scattered from ~ 50 to ~ 450 ms, showing thick and thin patches, between 38.5° N and 39.3° N. The sediments near the trench axis at around 38.6° N were thick due to the deposition of graben and trench fills (HDMY073; Fig. 4b), whereas those at ~ 38.8° N were thinner where the sediments of SU2 onlapped on the basement with abnormally rugged topography (HDMY101; Fig. 4a). At 39.3°–39.7° N, the sediments were very thin, mostly thinner than 200 ms. In addition, they were < 50 ms at some locations, as described previously (Fujie et al. 2020; Nakamura et al. 2020), where petit-spot activity (Hirano et al. 2006) is thought to have altered the incoming sediments and reduced apparent sediment thickness (Fujie et al. 2020). If the sill intruded into the sediments or altered sediments exist within SU2, they could create large acoustic impedance change and strong reflection which masks underlying structure. The actual bottom of the SU2 could not be imaged using our seismic data in such cases. The real sediment thickness including altered SU2 was probably not properly estimated in this area. At the northern end of the trench, 39.7°–40.7° N, sediments were thicker, 350–500 ms (e.g., HDSR219;

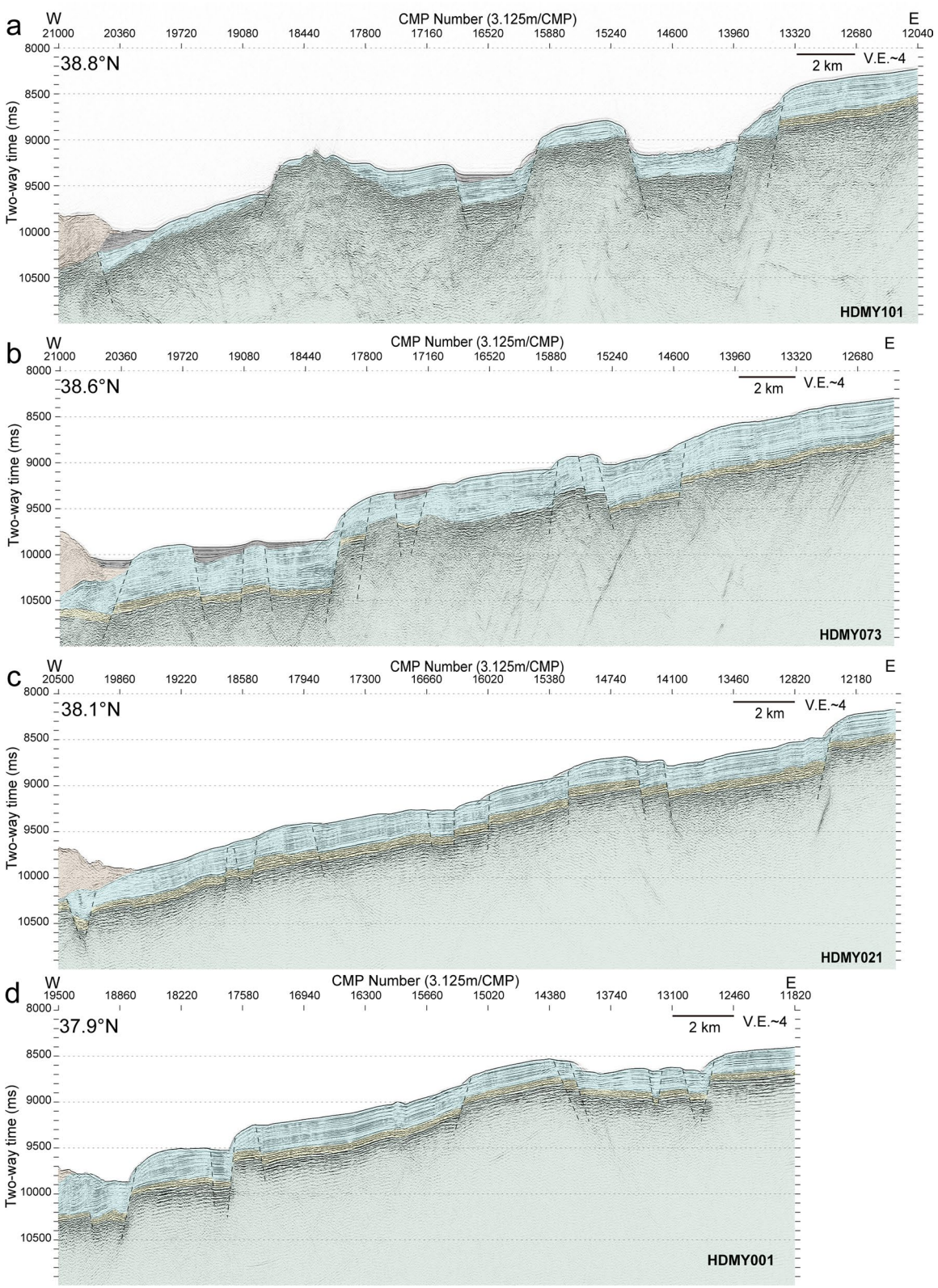

Fig. 4 Selected seismic profiles in the central part of the Japan Trench. Poststack time-migrated profiles with interpretation are shown. Brown, blue, yellow, and green shadings indicate seismic units SU1, SU2, SU3, and SU4, respectively. Gray shading indicates interpreted sediment fills. Bending-related normal faults are drawn with black dashed lines. The location of each profile is shown in Fig. 1

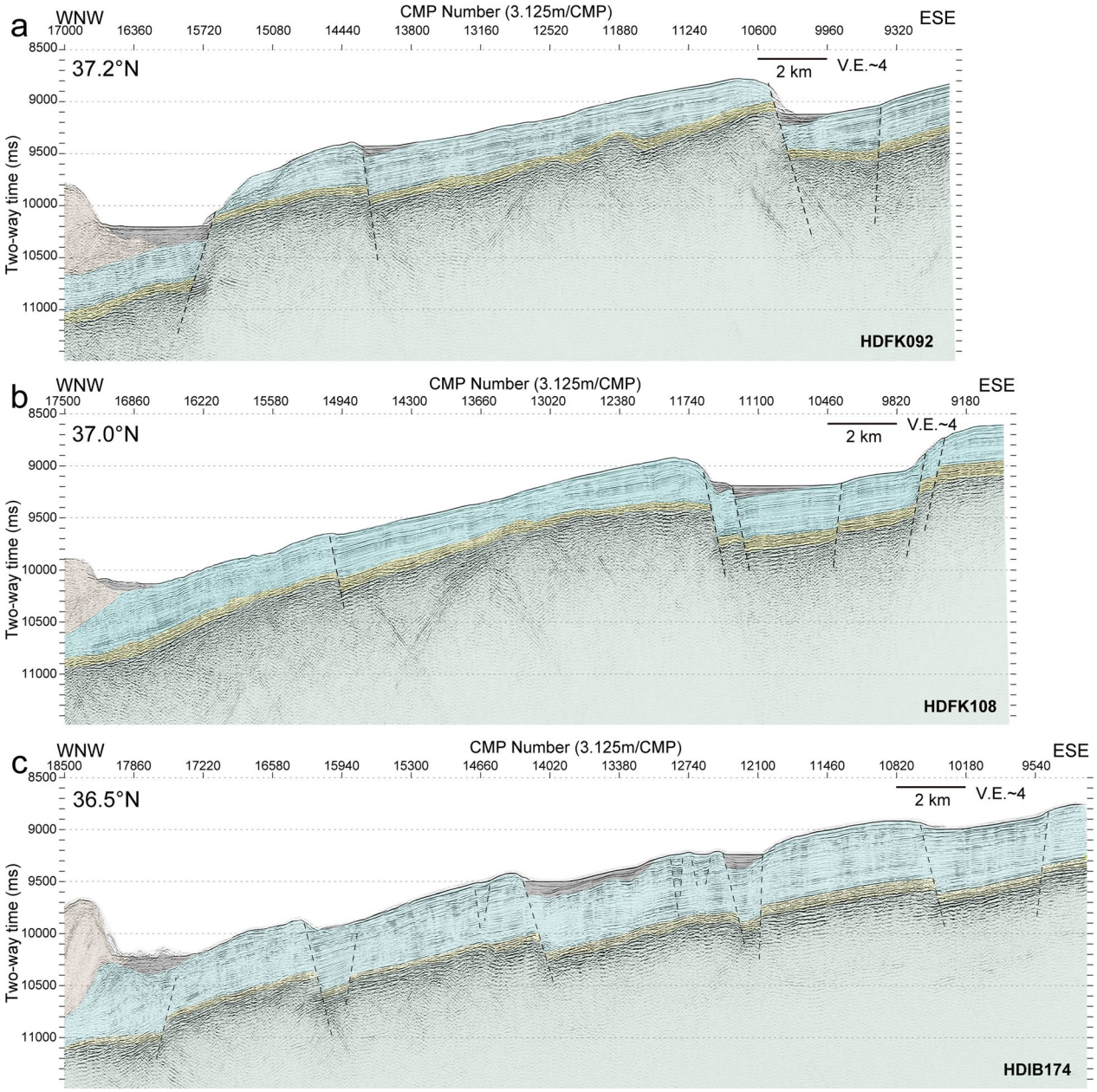

Fig. 5 Selected seismic profiles in the southern part of the Japan Trench. Poststack time-migrated profiles with interpretation are shown. Brown, blue, yellow, and green shadings indicate seismic units SU1, SU2, SU3, and SU4, respectively. Gray shading indicates interpreted sediment fills. Bending-related normal faults are drawn with black dashed lines. The location of each profile is shown on Fig. 1

(See figure on next page.)

Fig. 6 Distribution map of bending-related normal faults. **a** Map of the entire Japan Trench. Areas within the black dashed rectangles are shown in panels b and c. **b** Enlarged map of the southern part of the Japan Trench. **c** Enlarged map of the central and northern parts of the Japan Trench. Red and blue triangles indicate eastward and westward dipping normal faults, respectively. Darker colors indicate larger fault throws. The background map is a gray-shaded bathymetric map. The yellow line indicates the base of the landward slope. The thin white lines are seismic lines, and the thick black lines indicate locations of the seismic profiles shown in Figs. 3, 4, 5. Magenta contours show the slip distribution during the Tohoku earthquake (from Iinuma et al. 2012), same as Fig. 1. Orange dashed lines with arrowheads indicate the three segments inferred in this study. The same figure with the red-relief image as the background map is shown in Additional file 3: Fig. S3

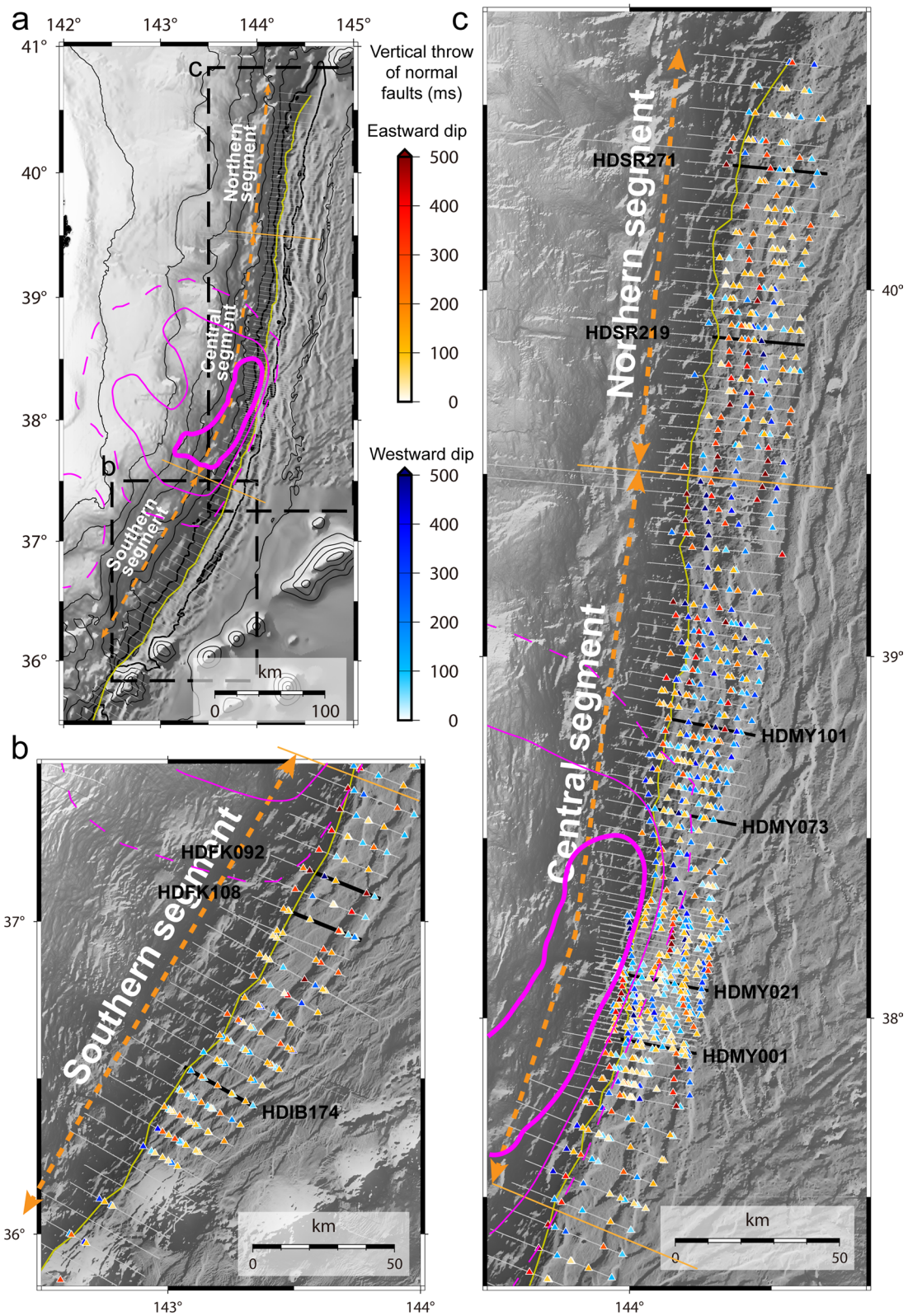

Fig. 6 (See legend on previous page.)

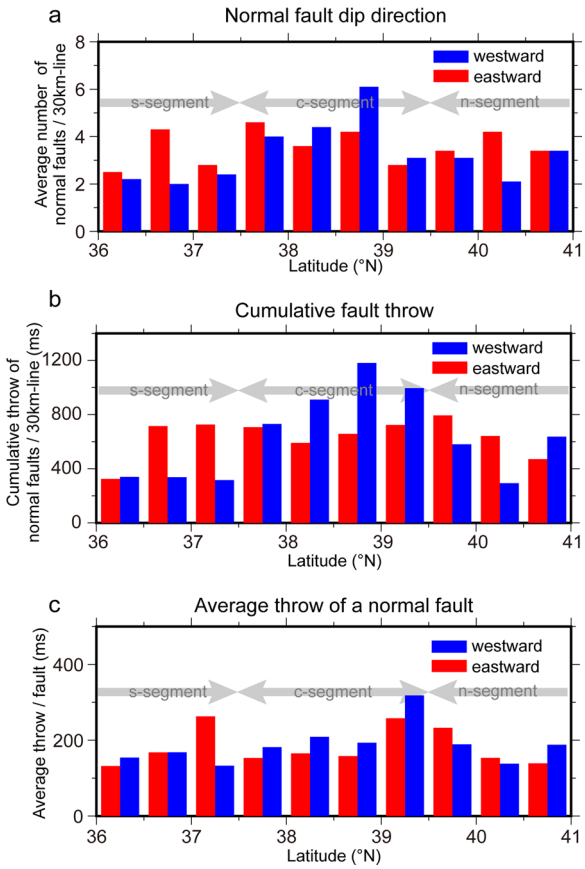

Fig. 7 Along-trench distribution of the dip direction and throw magnitude of the normal faults. **a** Average number of normal faults along a 30 km-long seismic line. The average number of the faults with eastward or westward dips along the seismic lines was estimated over every 0.5° of latitude. **b** The average cumulative throw along a 30 km-long seismic line. The average cumulative throw of eastward or westward dipping faults along the seismic lines was estimated over every 0.5° of latitude. **c** Average throw of a single fault. The average throw of eastward or westward dipping faults was estimated over every 0.5° of latitude. In all cases, normal faults with a vertical throw of > 50 ms were counted. Red and blue bars indicate eastward and westward dipping normal faults, respectively. Gray lines with arrowheads indicate the three segments inferred in this study. "s-segment," "c-segment," and "n-segment" denotes southern, central, and northern segment, respectively

Fig. 3b), and north of 40.1° N (e.g., HDSR271; Fig. 3a) the sediments around the trench axis were thicker than 550 ms.

Thus, in general, the thickness of the incoming sediments was 200–500 ms along the Japan Trench, but apparently thinner or thicker sediments were observed in some locations.

3.4 Sediment fills

Figure 9 shows the distribution and thickness of the interpreted graben- and trench-fill sediments. In the southern segment of the Japan Trench at 36°–37.5° N, trench fills are observed along most of the survey lines (Fig. 5a, c), and at 37°–37.5° N the thickness of the trench fill is greater than 200 ms (Fig. 5a). Graben fills have been deposited at 36.3°–36.5° N, north of the Katori seamount, where the total sediment thickness is especially great (Fig. 8). Graben fills at 36.8°–37.1° N occupy a well-developed NE–SW-trending graben. In the central part of the Japan Trench, trench and graben fills are fewer and their thickness is generally less than 100 ms at 37.8°–38.5° N. However, trench fills are moderately thick (~ 150–200 ms) around 38.5°–38.9° N (Fig. 4b). In the region between 37.8° and 38.9° N, graben fills are seen in isolated grabens, for example, a graben at ~ 38.3° N and two grabens at ~ 37.8° N. Trench fills are thick at ~ 39.3°–39.5° N (Nakamura et al. 2020). At ~ 39.5°–40° N, N–S-trending grabens with graben fills are seen east from the trench (Fig. 3b). In the northernmost part, north of 39.9° N, trench fills are observed along most of the survey lines (Fig. 3a), and graben fills are intermittently distributed from near the trench to the outer rise. The grabens are not well connected, probably as a result of influence from normal faults with ENE–WSW orientation that have developed along the Kuril Trench in this area.

Some sediment fills identified in the Japan Trench region show clear coherent, horizontal/sub-horizontal, parallel/sub-parallel stratification with relatively high amplitude (Type-A), whereas others show less coherent or wavy reflection with low amplitude (Type-B) (see also Fig. 10e and f). Many of the graben fills are Type-A (colored magenta in Figs. 10 and 11): for example, along Line HDFK076 (Fig. 10a), Line HDMY025 (Fig. 10b), and Line HDSR211 (around CMP 19000, Fig. 10c). Some Type-B graben fills (colored orange in Figs. 10 and 11) are observed: for example, along Line HDMY037 (Fig. 10d) and Line HDSR211 (around CMP 17000, Fig. 10c). Both

(See figure on next page.)

Fig. 8 Input sediment thickness. The vertical thickness of sediment above SU3 and SU4 was estimated based on the interpretation of each seismic profile (color scale). Along each profile, the western edge of the mapped sediment thickness is the deformation front or the base of the landward slope. Thin black lines indicate the seismic lines, and the thick black lines indicate seismic profiles shown in Figs. 3, 4, 5. Magenta contours show the slip distribution during the Tohoku earthquake (Iinuma et al. 2012), same as Fig. 1. The yellow thick dashed rectangles are the areas where the chert (SU3) is apparently missing (from Fujie et al. 2020), same as Fig. 1. The background map is a gray-shaded bathymetric map with contours every 200 m. The thick black contour line denotes a water depth of 7000 m. Orange dashed lines with arrowheads indicate the three segments inferred in this study. Similar thickness map without sediment fills (only SU2) is shown as Additional file 1: Fig. S1

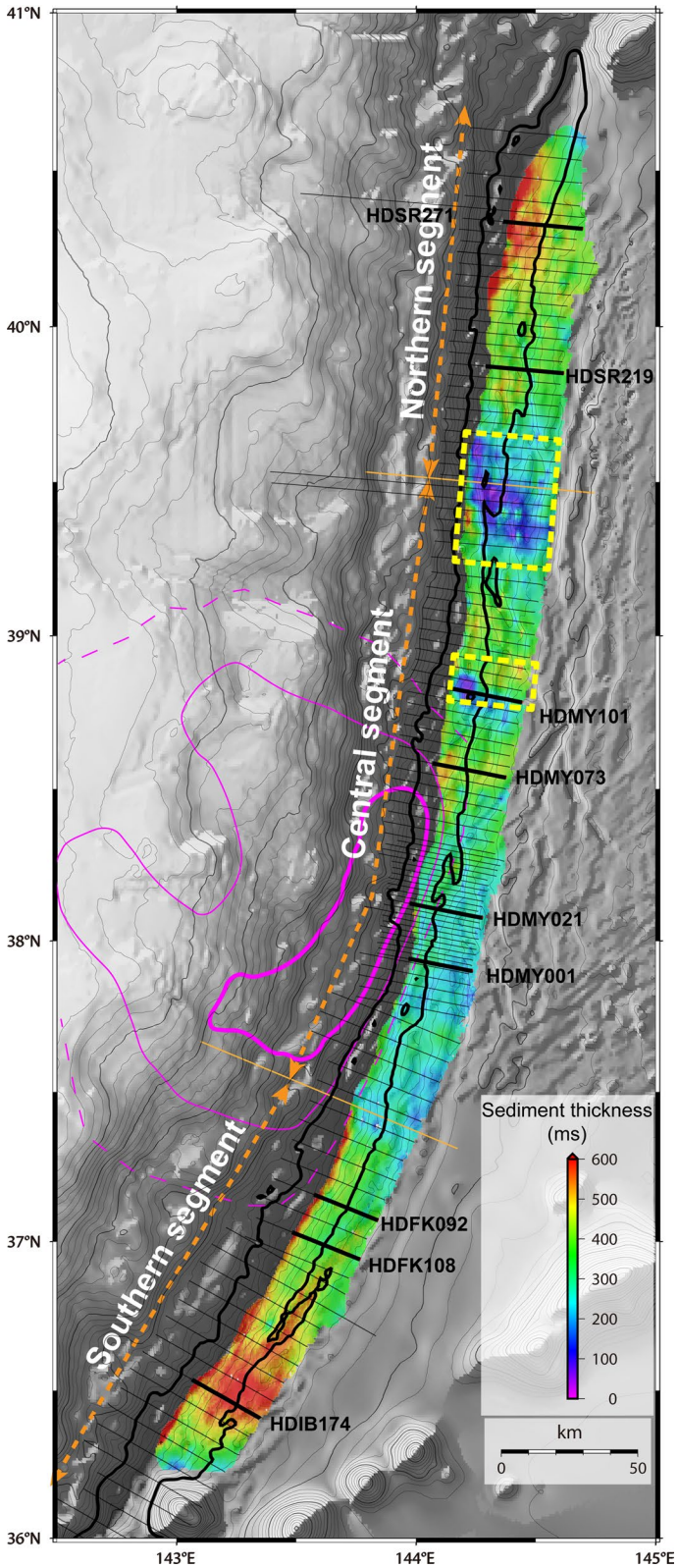

Fig. 8 (See legend on previous page.)

Type-A and Type-B trench fills are also observed. The trench fill along Line HDSR155 (Fig. 11a) is Type-B, whereas those along Line HDMY093 (Fig. 11b) and Line HDFK036 (Fig. 11c) are Type-A. We also observed the trench fills with both characteristics; for example, along Line HDFK060 Type-A trench-fill sediments underlie Type-B trench fill sediments (Fig. 11d), and along Line HDSR279, Type-B trench fill sediments are interbedded between Type-A trench fill sediments (Fig. 11e).

4 Discussion

4.1 Sediment input and great subduction zone earthquakes

A relationship between the thickness of incoming sediments in subduction zones and great subduction zone earthquakes has often been observed (e.g., Heuret et al. 2012). The thickness of the incoming sediments to the Japan Trench has been inferred to be 400–1200 m (Heuret et al. 2012) by referring to old seismic data (e.g., Ludwig et al. 1966; Lallemand et al. 1994). The average thickness of the incoming sediments along each survey line shows along-axis variation (Fig. 12). Our results clearly show that the average thickness of the incoming sediments is around 200–500 ms (about 160–500 m, assuming an average P-wave velocity of 1.6–2.0 km/s in the incoming sediments) in most of the Japan Trench. Although in some regions of the trench the maximum sediment thickness is up to about 700–950 ms (560–950 m, see Additional file 2: Fig. S2), the maximum incoming sediment thickness along each seismic line is 300–600 ms (240–600 m, Additional file 2: Fig. S2) at most of the Japan Trench. Thick incoming sediments in subduction zones generally create conditions preferable for hosting great earthquakes (e.g., Heuret et al. 2012; Brizzi et al. 2020) because they can potentially accommodate a smoother plate boundary fault interface, which promotes rupture propagation. As we demonstrated here, however, in the Japan Trench, the input sediments are relatively thin and there is distinct topographic relief on the incoming plate. In particular, sediment thickness is moderate (neither very thin nor thick), 200–350 ms (160–350 m) where the large slip occurred during the 2011 Tohoku earthquake (See also Fig. 1). This finding apparently contradicts the inferred relationship between sediment thickness and great earthquakes and suggests that to explain the generation of the large, shallow megathrust slip during the 2011 Tohoku earthquake, specific causes must be sought, as pointed out previously, such as the thermal pressurization (e.g., Noda and Lapusta 2013) and clay-rich plate boundary conditions (Chester et al. 2013; Ujiie et al. 2013).

4.2 Sediment fills

Sediment fills in the subduction zone could be turbidites (e.g., Nankai Trough; Ike et al. 2008). In the Japan Trench, recent studies reported the existence of earthquake-triggered turbidites ("seismo-turbidites") in the trench axis (e.g., Ikehara et al. 2016; Kioka et al. 2019; Schwestermann et al. 2021). They mainly consist of diatomaceous muds with coarse silt or sand at their bottom (Ikehara et al. 2016). The surface sediments on the landward slope were unstabilized by the earthquake and transported by the turbidity current through the canyons (e.g., Ogawara, Yamada, Nakaminato canyons; Fig. 1) to the trench. These canyons are not well developed like those in the Nankai Trough (Shimamura 2008), but the flow accumulation analysis showed a significant amount of flow along canyons on the Japan Trench landward slope (Kioka et al. 2019). The core sample analysis and sub-bottom profiler data showed that each seismo-turbidite has generally < 5 m of thickness and there are at least 2–4 turbidite units beneath the Japan Trench floor (Ikehara et al. 2016; Kioka et al. 2019). These turbidites show seismically transparent characteristics (Kioka et al. 2019). It is difficult to distinguish each turbidite in our seismic profiles because the dominant frequency in our data is ~ 50 Hz. The terrigenous sediments which could cause strong reflections were not transported into the Japan Trench axis unlike the Nankai Trough. However, the alternation of the turbidites and background sediments could be imaged as stratified (Type-A) trench fills on our seismic profiles. The Type-A graben fills are also observed on the seaward trench slope (outer rise) on the incoming plate. The grabens on the outer rise of the Japan Trench are isolated from the trench axis by horst blocks, and the water depth is shallower than the trench axis. The graben fills have not been studied with sediment cores so far. The origin and depositional process of the Type-A graben fill in the Japan Trench are still unknown. We note that the topmost sediments along Line HDFK060 have been

(See figure on next page.)

Fig. 9 Distribution of sediment fills. **a** Map for the entire Japan Trench. The areas within the black dashed rectangles are shown in panels b and c. **b** Enlarged map of the southern part of the Japan Trench. **c** Enlarged map of the central and northern parts of the Japan Trench. Distribution and thickness of the graben and trench fills are shown (color scale). Note that the range of the color scale is different from that for total sediment thickness (Fig. 8). The background map is a gray-shaded bathymetric map. The yellow line indicates the base of the landward slope. The thin white lines indicate the seismic lines, and the thick black lines indicate the seismic profiles shown in Figs. 10 and 11. Magenta contours show the slip distribution during the Tohoku earthquake (Iinuma et al. 2012), same as Fig. 1. Orange dashed lines with arrowheads indicate the three segments inferred in this study. The same figure with the red-relief image as the background map is shown in Additional file 4: Fig. S4

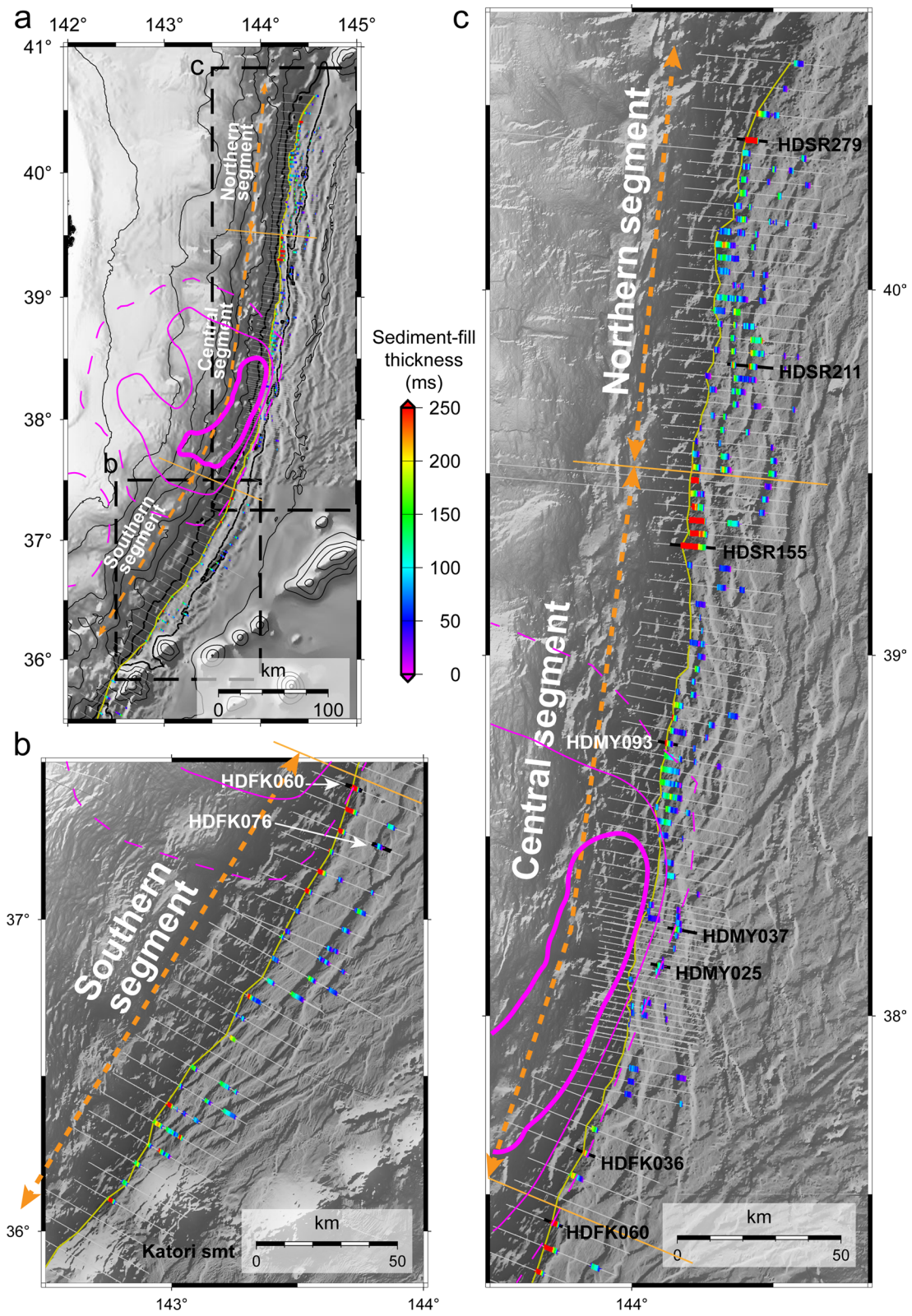

Fig. 9 (See legend on previous page.)

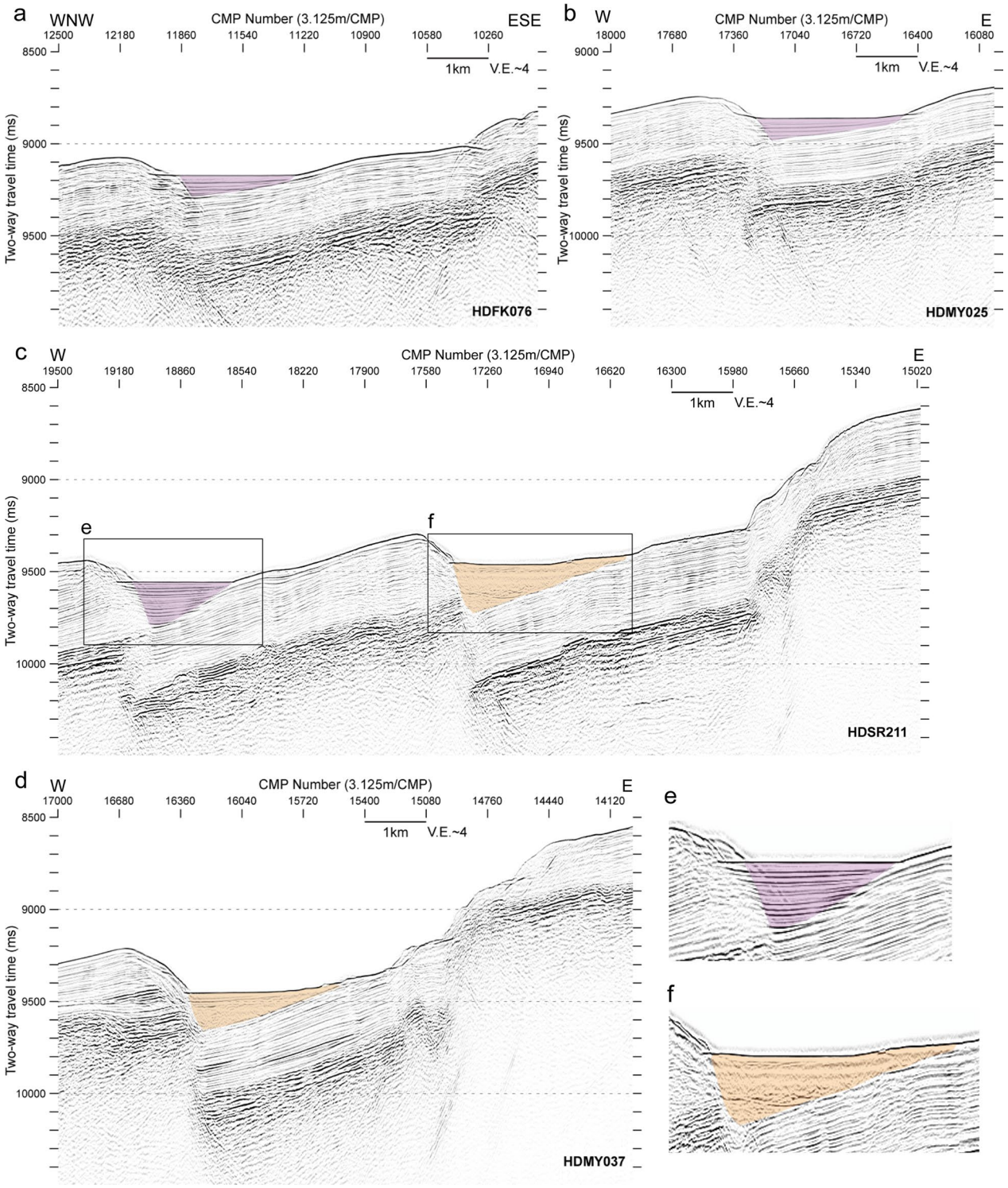

Fig. 10 Selected seismic profiles showing graben fills. Graben fills are observed in **a** Line HDFK076, **b** Line HDMY025, **c** Line HDSR211, and **d** Line HDMY037. Enlarged figures of the grabens in HDSR211 (**c**) are shown as (**e**) and (**f**) with amplified images. Magenta and orange indicate graben fills interpreted as Type-A and Type-B, respectively. The profile locations are shown in Fig. 9

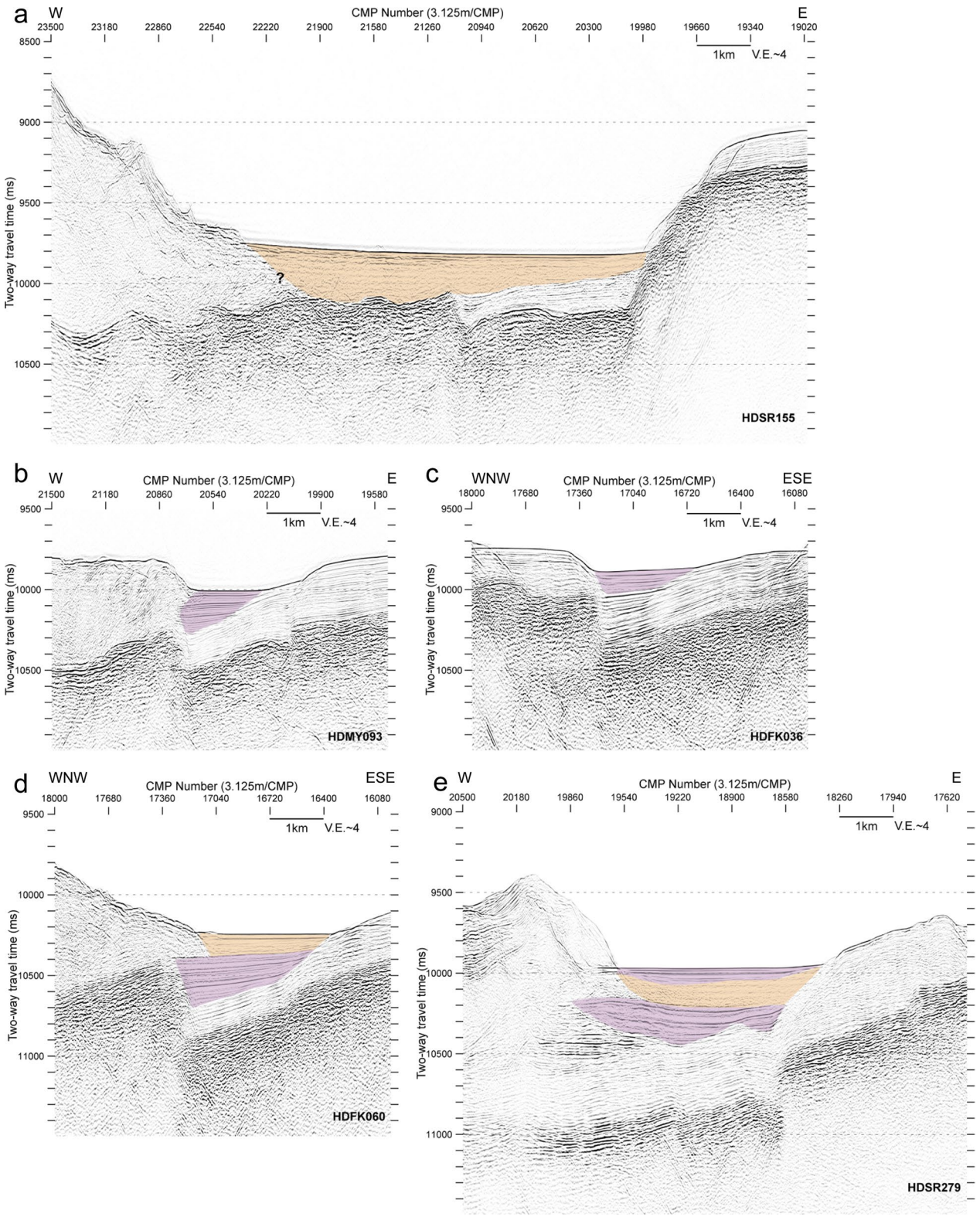

Fig. 11 Selected seismic profiles showing trench fills. Magenta and orange indicate trench fills interpreted as Type-A and Type-B, respectively. The profile locations are shown in Fig. 9

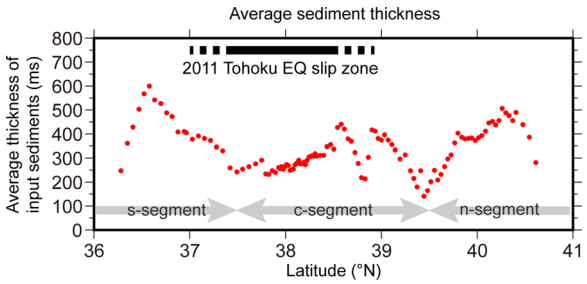

Fig. 12 Average thickness of the input sediments. The average thickness along each seismic line was calculated and plotted against the latitude of the line at the trench axis. The thickness was averaged from the eastern end to the deformation front of each seismic line. Gray lines with arrowheads indicate the three segments inferred in this study. "s-segment," "c-segment," and "n-segment" denotes southern, central, and northern segment, respectively

eroded at the western side of a knoll (Fig. 13). This observation suggests the remobilization of surface sediments. The nature of this knoll has not been investigated. The erosion of the surface sediments here might be related to the bottom current associated with the North Pacific Deep Water reported in the Japan Trench region (Mitsuzawa et al. 1995; Lee and Ogawa 1998). Although we did not observe clear indications like sediment waves or drifts, we speculate that the bottom current might have remobilized the surface sediments on the outer rise.

Another type of sediment fills (Type-B) is observed both in the trench axis and in grabens on the outer rise. Notable amounts of the trench-fill sediments were likely derived from slope failures and landslides along the landward trench slope (e.g., Strasser et al. 2013; Nakamura et al. 2020). Such non-stratified sediment fills (Type-B) are observed at 37°–37.5° N (e.g., along Line HDFK060; Fig. 11d), 39.3°–39.5° N (e.g., along Line HDSR155; Fig. 11a), 40.5° N (e.g., along Line HDSR279; Fig. 11e), areas outside of the large coseismic slip area of the 2011 Tohoku earthquake. The steep (10°–20°) inner walls of the trench at these locations suggest that failure of the lowermost landward slope may have occurred. Such slope failures might cause tsunamis.

Some of the graben fills show non-stratified seismic characteristics (Type-B). The existence of possible slope failures on normal fault scarps in the vicinity of the Type-B graben fills (Fig. 14) strongly suggests that these graben fills were produced by slope failures. Seafloor scarps are observed to the north of Type-B graben fills along Line HDSR211 in the northern Japan Trench. In addition, the estimated source region of the 1933 Showa Sanriku earthquake was in the outer rise area of the northern Japan Trench (e.g., Kanamori 1971; Uchida et al. 2016, see also Fig. 1). Thus, slope failures of these scarps might have been caused by strong ground motion during outer rise earthquakes.

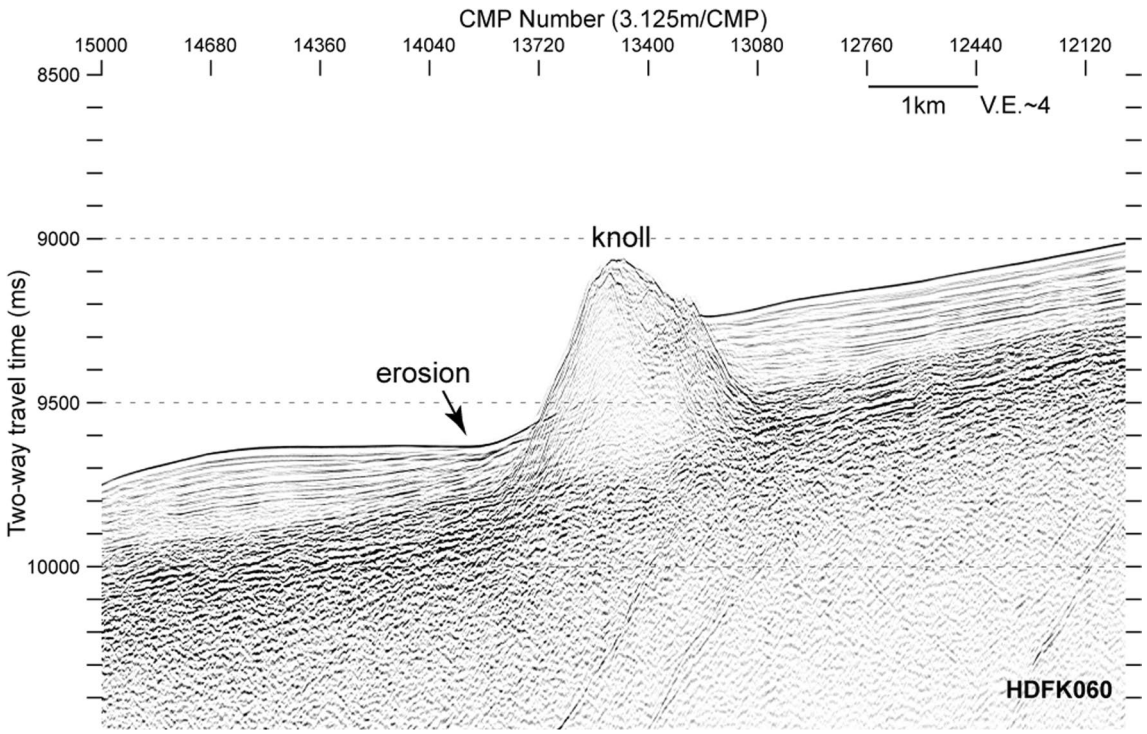

Fig. 13 Seismic profile of Line HDFK060. Surface erosion is observed west of a knoll located on this seismic line

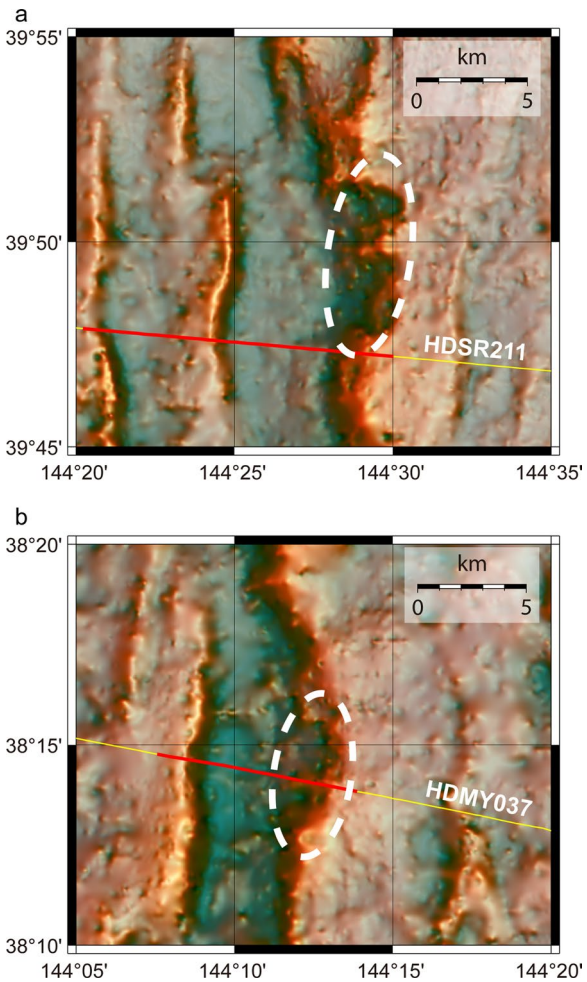

Fig. 14 Red-relief image maps (Chiba et al. 2008; Ohira et al. 2018) around **a** Line HDSR211 and **b** Line HDMY037. The seismic profiles denoted by the red lines are shown in Fig. 10c and d. The white dashed ellipses indicate interpreted scarp on the red-relief image

As discussed above, the graben- and trench-fill sediments deposited in the Japan Trench region probably originated from the remobilization or redistribution of the shallow seafloor sediments. Where they are deposited, the sediment fills increase the thickness of the input sediments with remobilized sediments.

4.3 Normal faults

Our results indicate that normal faults with westward (trenchward) and eastward (oceanward) dip directions have developed in comparable number along the Japan Trench (Fig. 7). Interestingly, however, eastward dipping normal faults occur more frequently than westward dipping faults in the northern and southern segments of the trench (Fig. 7a, b), which means that many westward dipping half-grabens occur in these regions. Nakanishi (2011) reported that asymmetric grabens, which are half-grabens tilted toward the trench, are topographically expressed in bathymetric data from the northern and southern parts of the Japan Trench. In the Middle America subduction zone, the incoming Cocos plate also has half-graben structures, but the normal faults mainly dip trenchward (e.g., Ranero et al. 2003). In the central part of the Japan Trench, the distributions of normal faults and fault strikes are complicated (Fig. 6); this complexity is probably related to the possible pseudofaults pointed out by Nakanishi (2011). Westward dipping faults are numerous at 38°–39° N, but ~ 40% of the normal faults are eastward dipping. In areas where eastward dipping normal faults are more numerous, the faults are linearly aligned either parallel to (north, 39.5°–40°N) or oblique to (south, 36.5°–37.5° N) the strike of the trench axis. The western edge of a westward-tilted graben bounded by an eastward dipping normal fault is well situated to accumulate sediments redeposited from original sediments in surrounding regions. The oceanward dipping faults are predominant in the Chilean subduction zone (Ranero et al. 2005), which is similar to our observation in the northern and southern segments in the Japan Trench. However, the thickness of the sediments is much thicker (> 1 km) in the Chilean subduction zone (Olsen et al. 2020) than in the Japan Trench (Fig. 8). The development of oceanward dipping faults with deposition of sediment fills over relatively thin sediments is a characteristic of the incoming structure to the Japan Trench.

The deposition of graben fills obscures the throw of the normal faults, especially those dipping eastward. The activity of the normal faults and their trenchward development have often been inferred only by using bathymetric data for the Japan Trench (Iwabuchi 2012, 2013); as a result, the throw of eastward dipping normal faults may have been underestimated. For example, the vertical throw of the normal fault around CDP 19180 on Line HDSR211 (Fig. 10c) has been estimated to be ~ 75 m from the bathymetry data; however, the actual throw, estimated from the seismic profile, is > 270 m (~ 340 ms of TWT). Iwabuchi (2012) reported that westward dipping normal faults are dominant along the entire Japan Trench. However, our results suggest that the numbers and cumulative throws of westward and eastward dipping normal faults are generally comparable, and that eastward dipping faults are actually dominant in the northern and southern segments of the trench (Fig. 7). We note that the coverage of the seismic lines in this study is not sufficient to discuss the development of normal faults over the entire extent of the outer rise. Careful consideration is necessary to infer the development and activity of the outer rise normal faults.

4.4 Correspondence to megathrust slip styles

Our results demonstrated that in the area between 37.5° and 38.5° N, where the large shallow slip during the 2011 Tohoku earthquake occurred, the thickness of the input sediments is moderately thick at 200–350 ms with less variation (Figs. 8, 12), without remarkable sediment fills (Fig. 9). The westward dipping faults are predominant (Figs. 7a, 7b), and the fault throws are small (Fig. 6) at ~ 150–200 ms on average (Fig. 7c), close to the thickness of the incoming sediments.

Outside of the large slip zone of the Tohoku earthquake to the north, the area between 38.5° and 39° N partially exhibits similar features with the large slip zone; e.g., westward dipping faults are more (Figs. 7a, 7b) and the throws of the normal faults are small (Fig. 7c). However, the thickness of the input sediments is variable (Figs. 8, 12) and trench fill sediments are observed (Fig. 9), which are different from the large slip zone. A small cluster of tremors and VLFEs were reported at 38.8°–38.9° N (Nishikawa et al. 2019; Fig. 1), where the basement with rugged topography and a thin sediment patch are observed in the incoming plate on our seismic profile (Line HDMY101; Figs. 4a, 8). This anomalous structure has a < 10 km horizontal scale.

Sporadic tremor and VLFE activities were observed in the area 39°–39.5° N (Nishikawa et al. 2019; Fig. 1). Although the sediment fills are observed (Fig. 9), the incoming plate has apparently thin sediments in this area, especially around 39.5° N (Figs. 8, 12). The apparent thinning of the sediments is related to the petit-spot activities (Hirano et al. 2006; Fujie et al. 2020). The throws of the normal faults become larger than other areas (Fig. 7c).

Further to the north, between 39.5° and 40.5° N, tremors and VLFEs are active (Nishikawa et al. 2019; Fig. 1). The thickness of the sediments is generally greater than 400 ms except for 39.5°–39.7° N (Fig. 12). Sediment fills are also observed in the trench axis and grabens (Fig. 9). The eastward dipping faults are predominant in this region (Figs. 7a, 7b), which provides the favorable condition for the deposition of the graben fills. Similar structural features are observed in the southern segment of the Japan Trench between 36.5° and 37.5° N. Tremors and VLFEs are observed between 36.5° and 37° N (Nishikawa et al. 2019; Fig. 1).

These observations are summarized as follows (Fig. 15). The large slip zone of the 2011 Tohoku earthquake corresponds to the area of the incoming plate with (1) moderate-thick (200–350 ms or 160–350 m) sediments with small thickness variation and (2) full-graben-type horst–graben structure with relatively small throws (150–200 ms or 120–200 m) of bending-related normal faults. On the other hand, areas outside the large slip zone show different characteristics in the incoming plate structure, e.g., very rugged topography of the basement such as petit-spots, dominance in the eastward dipping normal faults, thicker sediments with large amount of sediment fills, or horizontally small-scale thickness variation of the sediment. The areas with thick sediments (> 400 ms or > 320–400 m) in the incoming plate correspond to the areas hosting tremors and VLFEs. The incoming plate with the rugged basement and apparently thinner sediments (< 100 ms or < 80–100 m) also corresponds to the areas where tremors and VLFE are observed.

As described above, we could observe a certain correspondence between the incoming structures and the

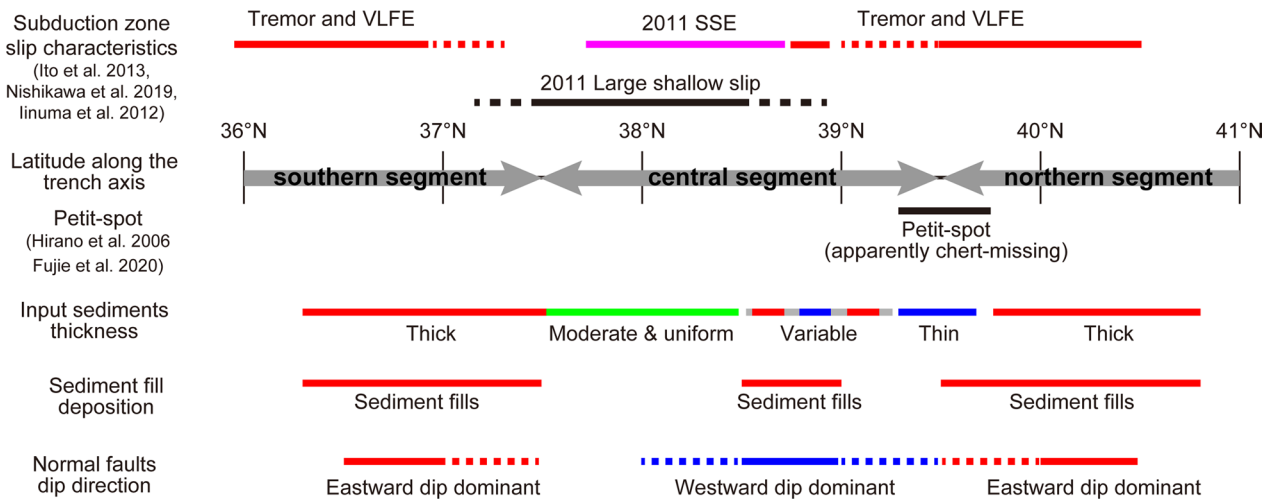

Fig. 15 Schematic diagram showing correspondences between the observed incoming plate structure and subduction zone slip behaviors. Gray lines with arrowheads indicate the three segments inferred in this study

megathrust slip style in the Japan Trench subduction zone. Subducting ridges or seamounts have been related to the slow earthquakes in the southern Japan Trench, Nankai Trough, and Hikurangi subduction zones. The rugged basement structure at ~ 38.8° N in this study has smaller dimensions than those of ridges or seamounts previously reported; however, such a small-scale basement relief may also contribute to the favorable condition for the tremors and VLFEs.

The areas with thick incoming sediments also correspond to the tremors and VLFEs in the northern and southern segments in the Japan Trench. The thick sediment inputs into the subduction zone may bring larger amount of underthrust sediments with fluid, which may increase the pore pressure in the megathrust and thus host favorable conditions for slow earthquakes. However, the location of the decollement in the Japan Trench subduction zone is complicated due to the subduction of the horst–graben structure, and it has not been well resolved in previous studies. In the central part of the Japan Trench, the trenchward tip of the decollement steps down into trench graben sediments (e.g., Kodaira et al. 2012; Nakamura et al. 2013; Boston et al. 2014). But the decollement level could be different after subduction, which bridges between horst blocks to shortcut the step-down in the graben (Jamali Hondori and Park 2022). When a graben in which incoming sediments and sediment fills are thick enough is situated at the trench axis, the decollement may not step down to the deeper level of graben sediments, because the stress condition at the graben edge may be different from the case of the trench graben with thin sediments (Boston et al. 2014; Martel and Langley 2006). In such case, the larger amount of incoming sediments might underthrust beneath the megathrust. Further studies are necessary to link thick incoming sediments to tremors and VLFEs in the Japan Trench subduction zone.

5 Summary

Sediment thickness and bending-related normal faults on the incoming Pacific plate to the Japan Trench were mapped by using more than 100 reflection profiles. The thickness of the sediments varies along the trench: The incoming sediment thickness averaged over each seismic line is mostly < 500 m, but the average sediment thickness is < 350 m where the most significant shallow slip occurred during the 2011 Tohoku earthquake. On the other hand, areas where thick incoming sediments are subducting correspond to areas, outside the large slip zone of the 2011 Tohoku earthquake, characterized by tremor and VLFE activity. The area with apparently very thin sediments related to petit-spot activities also corresponds to the tremor-VLFE-prone area. Additionally, a horizontally small-scale basement relief corresponds to a small cluster of the tremors and VLFEs. Bending-related normal faults offset the sediments and basement of the Pacific plate. Unlike the case at the Middle America Trench, eastward (oceanward) dipping normal faults have been developed comparably well to westward (trenchward) dipping faults along the entire Japan Trench, and they are predominant in its northern and southern segments. The deposition of sediment fills associated with eastward dipping normal faults leads to underestimation of the throws of those faults. Sediment-fill deposition increases the sediment inputs into the subduction zone, which may cause the favorable condition to host tremors and VLFEs. Along-axis variation of the incoming plate structure corresponds to the variation of the megathrust slip behaviors in the Japan Trench, but further studies are necessary to establish a linkage between the input structure and megathrust slip behaviors in the subduction zone.

Abbreviations

JAMSTEC	Japan Agency for Marine-Earth Science and Technology
TWT	Two-way travel time
VLFE	Very low-frequency earthquake
V. E.	Vertical exaggeration

Supplementary Information

The online version contains supplementary material available at https://doi.org/10.1186/s40645-023-00579-7.

Additional file 1. Fig. S1: Thickness of the SU2 without sediment fills. Vertical thickness of SU2 is shown in this map. Other legends and remarks are the same as Fig. 8.

Additional file 2. Fig. S2 Maximum thickness of input sediments. Same as Fig. 12, except the maximum value of the input sediment thickness on each seismic line is plotted.

Additional file 3. Fig. S3 Distribution map of bending-related normal faults on the red-relief map. Same as Fig. 6 but uses the red-relief image as the background map. Green dashed lines with arrowheads indicate the three segments inferred in this study.

Additional file 4. Fig. S4 Distribution of sediment fills on the red-relief map. Same as Fig. 9 but uses the red-relief image as the background map. Green dashed lines with arrowheads indicate the three segments inferred in this study.

Acknowledgements

The authors are grateful to Prof. Ryota Hino, Prof. Ryuji Tada, Prof. Michael Strasser, and an anonymous reviewer for their valuable comments which helped to improve the manuscript. We thank captains H. Tanaka, E. Ukekura, T. Inoue, Y. Nakamura, and S. Ryono and the crews of R/V *Kairei*, R/V *Kaiyo*, and R/V *Yokosuka* for the safe and kind operation on the ships, and M. Ito, Y. Ohwatari, H. Shibata, and marine technicians for their technical support during the seismic surveys. Figures 1, 6, 7, 8, 9, 12, 14, Additional files 1, 3, 4: Fig. S1, S3, and S4 were created with Generic Mapping Tools 6 (Wessel et al. 2019). Bathymetry data from Kido et al. (2011), JHOD, JAMSTEC (2011), and Olson et al. (2016) were used to prepare the detailed bathymetric and red-relief maps.

Author contributions
YN participated in all the seismic cruises, processed and interpreted the seismic data, and wrote the manuscript. SK managed the project and contributed to the interpretation. GF participated in the data acquisition and helped to develop the discussion. MY and KO participated in the data acquisition. SM managed and supported the project and the planning of the seismic cruises. All authors read and approved the final manuscript.

Funding
This work was supported by JSPS KAKENHI Grant Numbers 26000002, 15H05718, 19H05596.

Availability of data and materials
The seismic datasets supporting the conclusions of this article are available in the JAMSTEC seismic survey database, https://doi.org/doi:10.17596/0002069.

Declarations

Competing interests
The authors declare that they have no competing interest.

Author details
[1]Japan Agency for Marine-Earth Science and Technology (JAMSTEC), 3173-25 Showa-Machi, Kanazawa-ku, Yokohama, Kanagawa 236-0001, Japan. [2]Present Address: Advanced Industrial Science and Technology, 1-1-1 Umezono, Tsukuba, Ibaraki 305-8560, Japan.

Received: 24 November 2022 Accepted: 27 July 2023
Published online: 08 August 2023

References

Baba S, Takeo A, Obara K, Matsuzawa T, Maeda T (2020) Comprehensive detection of very low frequency earthquakes off the Hokkaido and Tohoku Pacific coasts, northeastern Japan. J Geophys Res 125(1):e2019JB017988. https://doi.org/10.1029/2019JB017988

Bassett D, Sandwell DT, Fialko Y, Watts AB (2016) Upper-plate controls on coseismic slip in the 2011 magnitude 9.0 Tohoku-oki earthquake. Nature 531(7592):92–96. https://doi.org/10.1038/nature16945

Boston B, Moore GF, Nakamura Y, Kodaira S (2014) Outer-rise normal fault development and influence on near-trench décollement propagation along the Japan Trench, off Tohoku. Earth Planets Space 66:135. https://doi.org/10.1186/1880-5981-66-135

Brizzi S, van Zelst I, Funiciello F, Corbi F, van Dinther Y (2020) How sediment thickness influences subduction dynamics and seismicity. J Geophys Res 125:e2019JB018964. https://doi.org/10.1029/2019JB018964

Chester FM, Rowe C, Ujiie K, Kirkpatrick J, Regalla C, Remitti F, Moore JC, Toy V, Wolfson-Schwehr M, Bose S, Kameda J, Mori JJ, Brodsky EE, Eguchi N, Toczko S, Expedition 343 and 343T Scientists (2013) Structure and composition of the plate-boundary slip zone for the 2011 Tohoku-Oki earthquake. Science 342:1208–1211. https://doi.org/10.1126/science.1243719

Chiba T, Kaneta S, Suzuki Y (2008) Red relief image map: new visualization method for three dimensional data. Int Arch Photogramm Remote Sens Spat Inf Sci 37(B2):1071–1076

Cloos M (1992) Thrust-type subduction-zone earthquakes and seamount asperities: a physical model for seismic rupture. Geology 20:601–604

Dragert H, Wang K, Rogers G (2004) Geodetic and seismic signatures of episodic tremor and slip in the northern Cascadia subduction zone. Earth Planets Space 56(12):1143–1150. https://doi.org/10.1186/BF03353333

Fujie G, Kodaira S, Sato T, Takahashi T (2016) Along-trench variations in the seismic structure of the incoming Pacific plate at the outer rise of the northern Japan Trench. Geophys Res Lett 43:666–673. https://doi.org/10.1002/2015GL067363

Fujie G, Kodaira S, Kaiho Y, Yamamoto Y, Takahashi T, Miura S, Yamada T (2018) Controlling factor of incoming plate hydration at the northwestern Pacific margin. Nat Commun 9:3844. https://doi.org/10.1038/s41467-018-06320-z

Fujie G, Kodaira S, Nakamura Y, Morgan JP, Dannowski A, Thorwart M, Grevemeyer I, Miura S (2020) Spatial variations of incoming sediments at the northeastern Japan arc and their implications for megathrust earthquakes. Geology. https://doi.org/10.1130/G46757.1

Heuret A, Conrad CP, Funiciello F, Lallemand S, Sandri L (2012) Relation between subduction megathrust earthquakes, trench sediment thickness and upper plate strain. Geophys Res Lett 39:L05304. https://doi.org/10.1029/2011GL050712

Hirano N, Takahashi E, Yamamoto J, Abe N, Ingle SP, Kaneoka I, Hirata T, Kimura J, Ishii T, Ogawa Y, Machida S, Suyehiro K (2006) Volcanism in response to plate flexure. Science. https://doi.org/10.1126/science.1128235

Hua Y, Zhao D, Toyokuni G, Xu Y (2020) Tomography of the source zone of the great 2011 Tohoku earthquake. Nat Commun 11:1163. https://doi.org/10.1038/s41467-020-14745-8

Ide S, Baltay A, Beroza GC (2011) Shallow dynamic overshoot and energetic deep rupture in the 2011 Mw 9.0 Tohoku-Oki earthquake. Science. https://doi.org/10.1126/science.1207020

Iinuma T, Hino R, Kido M, Inazu D, Osada Y, Ito Y, Ohzono M, Tsushima H, Suzuki S, Fujimoto H, Miura S (2012) Coseismic slip distribution of the 2011 off the Pacific Coast of Tohoku Earthquake (M9.0) refined by means of seafloor geodetic data. J Geophys Res 117:B07409. https://doi.org/10.1029/2012JB009186

Ike T, Moore GF, Kuramoto S, Park JO, Kaneda Y, Taira A (2008) Variations in sediment thickness and type along the northern Philippine Sea Plate at the Nankai Trough. Island Arc 17:342–357. https://doi.org/10.1111/j.1440-1738.2008.00624.x

Ikehara K, Kanamatsu T, Nagahashi Y, Strasser M, Fink H, Usami K, Irino T, Wefer G (2016) Documenting large earthquakes similar to the 2011 Tohoku-oki earthquake from sediments deposited in the Japan Trench over the past 1500 years. Earth Planet Sci Lett 445:48–56. https://doi.org/10.1016/j.epsl.2016.04.009

Ito Y, Obara K (2006) Very low frequency earthquakes within accretionary prisms are very low stress-drop earthquakes. Geophys Res Lett. https://doi.org/10.1029/2006GL025883

Ito Y, Hino R, Kido M, Fujimoto H, Osada Y, Inazu D, Ohta Y, Iinuma T, Ohzono M, Miura S, Mishina M, Suzuki K, Tsuji T, Ashi J (2013) Episodic slow slip events in the Japan subduction zone before the 2011 Tohoku-Oki earthquake. Tectonophysics 600:14–26. https://doi.org/10.1016/j.tecto.2012.08.022

Iwabuchi Y (2012) Extension rates in the outer slope of Japan Trench derived from precise seabottom topographies (in Japanese with English abstract). Zisin 65:9–19. https://doi.org/10.4294/zisin.65.9

Iwabuchi Y (2013) Developed tectonic relief and frequency of great earthquake caused by normal faults in the outer slope of the Japan Trench (in Japanese with English abstract). Rep Hydrogr Oceanogr Res 50:1–24

Jamali Hondori E, Park JO (2022) Connection between high pore-fluid pressure and frictional instability at tsunamigenic plate boundary fault of 2011 Tohoku-Oki earthquake. Sci Rep 12:12556. https://doi.org/10.1038/s41598-022-16578-5

JHOD, JAMSTEC (2011) Bathymetry data off Tohoku, Japan (in Japanese). Seismol Soc Jpn News Lett 23(2):35–36

Kanamori H (1971) Seismological evidence for a lithospheric normal faulting: the Sanriku earthquake of 1933. Phys Earth Planet Interiors 4:289–300

Kido Y, Fujiwara T, Sasaki T, Kinoshita M, Kodaira S, Sano M, Ichiyama Y, Hanafusa Y, Tsuboi S (2011) Bathymetric feature around Japan Trench obtained by JAMSTEC multi narrow beam survey. Abstract MIS036-P58 presented at Japan Geoscience Union Meeting 2011, Chiba, Japan, 20–25 May 2011

Kioka A, Schwestermann T, Moernaut J, Ikehara K, Kanamatsu T, Eglinton TI, Strasser M (2019) Event stratigraphy in a Hadal Oceanic Trench: The Japan Trench as sedimentary archive recording recurrent giant subduction zone earthquakes and their role in organic carbon export to the deep sea. Front Earth Sci 7:319. https://doi.org/10.3389/feart.2019.00319

Kodaira S, No T, Nakamura Y, Fujiwara T, Kaiho Y, Miura S, Takahashi N, Kaneda Y, Taira A (2012) Coseismic fault rupture at the trench axis during the 2011 Tohoku-oki earthquake. Nature Geosci 5:646–650. https://doi.org/10.1038/NGEO1547

Kodaira S, Nakamura Y, Yamamoto Y, Obana K, Fujie G, No T, Kaiho Y, Sato T, Miura S (2017) Depth-varying structural characters in the rupture zone of the 2011 Tohoku-oki earthquake. Geosphere 13:1408–1424. https://doi.org/10.1130/GES01489.1

Lallemand SE, Schnurle P, Malavieille J (1994) Coulomb theory applied to accretionary and nonaccretionary wedges: Possible causes for tectonic erosion and/or frontal accretion. J Geophys Res 99:12033–12055

Lay T (2018) A review of the rupture characteristics of the 2011 Tohoku-oki Mw 9.1 earthquake. Tectonophysics 733:4–36. https://doi.org/10.1016/j.tecto.2017.09.022
Lee IT, Ogawa Y (1998) Bottom-current deposits in the Miocene-Pliocene Misaki Formation, Izu forearc area, Japan. Island Arc 7:315–329. https://doi.org/10.1111/j.1440-1738.1998.00192.x
Ludwig WJ, Ewing JI, Ewing M, Murauchi S, Den N, Asano S, Hotta H, Hayakawa M, Asanuma T, Ichikawa K, Noguchi I (1966) Sediments and structure of the Japan Trench. J Geophys Res 71:2121–2137
Martel SJ, Langley JS (2006) Propagation of normal faults to the surface in basalt, Koae fault system. Hawaii J Struct Geol 28(12):2123–2143. https://doi.org/10.1016/j.jsg.2005.12.004
Mitsuzawa K, Momma H, Horiuchi K, Miyamoto M, Aoki M (1995) Measurement of bottom current in deep-sea of far-off the Sanriku, Japan Trench (Abstract in Japanese). JAMSTEC 11th Deep Sea Symposium, Tokyo 155
Mochizuki K, Yamada T, Shinohara M, Yamanaka Y, Kanazawa T (2008) Weak interplate coupling by seamounts and repeating M ~ 7 earthquakes. Science 321(5893):1194–1197. https://doi.org/10.1126/science.1160250
Nakamura Y, Kodaira S, Miura S, Regalla C, Takahashi N (2013) High-resolution seismic imaging in the Japan Trench axis area off Miyagi, northeastern Japan. Geophys Res Lett 40:1713–1718. https://doi.org/10.1002/grl.50364
Nakamura Y, Fujiwara T, Kodaira S, Miura S, Obana K (2020) Correlation of frontal prism structures and slope failures near the trench axis with shallow megathrust slip at the Japan Trench. Sci Rep 10:11607. https://doi.org/10.1038/s41598-020-68449-6
Nakanishi M (2011) Bending-related topographic structures of the subducting plate in the Northwestern Pacific Ocean. In: Ogawa Y et al. (eds) Accretionary prisms and convergent margin tectonics in the Northwest Pacific Basin, Modern approaches in solid earth sciences. https://doi.org/10.1007/978-90-481-8885-7_1
Nishikawa T, Matsuzawa T, Ohta K, Uchida N, Nishimura T, Ide S (2019) The slow earthquake spectrum in the Japan Trench illuminated by the S-net seafloor observatories. Science 365:808–813. https://doi.org/10.1126/science.aax5618
Nishikawa T, Ide S, Nishimura T (2023) A review on slow earthquakes in the Japan Trench. Prog Earth Planet Sci 10:1. https://doi.org/10.1186/s40645-022-00528-w
Nishimura T (2021) Slow slip events in the Kanto and Tokai regions of central Japan detected using global navigation satellite system data during 1994–2020. Geochem Geophys Geosyst 22(2):e2020GC009329. https://doi.org/10.1029/2020GC009329
Noda H, Lapusta N (2013) Stable creeping fault segments can become destructive as a result of dynamic weakening. Nature 493:518–521. https://doi.org/10.1038/nature11703
Obana K, Fujie G, Yamamoto Y, Kaiho Y, Nakamura Y, Miura S, Kodaira S (2021) Seismicity around the trench axis and outer-rise region of the southern Japan Trench, south of the main rupture area of the 2011 Tohoku-oki earthquake. Geophys J Int 226(1):131–145. https://doi.org/10.1093/gji/ggab093
Ohira A, Kodaira S, Fujie G, No T, Nakamura Y, Kaiho Y, Miura S (2018) Seismic structure of the oceanic crust around petit-spot volcanoes in the outer-rise region of the Japan Trench. Geophys Res Lett 45:11–23. https://doi.org/10.1029/2018GL080305
Olsen KM, Bangs NL, Trehu AM, Han S, Arnulf A, Cotreras-Reyes E (2020) Thick, strong sediment subduction along south-central Chile and its role in great earthquakes. Earth Planet Sci Lett 538:116195. https://doi.org/10.1016/j.epsl.2020.116195
Olson CJ, Becker JJ, Sandwell DT (2016) SRTM15 PLUS: data fusion of Shuttle Radar Topography Mission (SRTM) land topography with measured and estimated seafloor topography (NCEI Accession 0150537). NOAA National Centers for Environmental Information. Accessed 9 Feb 2021, https://www.ncei.noaa.gov/archive/accession/0150537
Qin Y, Nakamura Y, Kodaira S, Fujie G (2022) Seismic imaging of subsurface structural variations along the Japan trench south of the 2011 Tohoku earthquake rupture zone. Earth Planet Sci Lett 594:117707. https://doi.org/10.1016/j.epsl.2022.117707
Ranero CR, Morgan JP, McIntosh K, Reichert C (2003) Bending-related faulting and mantle serpentinization at the Middle America trench. Nature 425:367–373. https://doi.org/10.1038/nature01961
Ranero CR, Villasenor A, Morgan JP, Weinrebe W (2005) Relationship between bend-faulting at trenches and intermediate-depth seismicity. Geochm Geophys Geosyst 6:Q12002. https://doi.org/10.1029/2005GC000997
Satake K, Fujii Y, Harada T, Namegaya Y (2013) Time and space distribution of coseismic slip of 2011 Tohoku Earthquake as inferred from tsunami waveform data. Bull Seismol Soc Am. https://doi.org/10.1785/0120120122
Schwestermann T, Eglinton TI, Haghipour N, McNichol AP, Ikehara K, Strasser M (2021) Event-dominated transport, provenance, and burial of organic carbon in the Japan Trench. Earth Planet Sci Lett 563:116870. https://doi.org/10.1016/j.epsl.2021.116870
Shimamura K (2008) Revised chart of the submarine canyon and valley systems around the Japanese Islands -on their topographic features and their unsettled questions- (in Japanese with English abstract). J Geol Soc Japan 114:560–576
Shipboard Scientific Party (1980) Site 436, Japan Trench Outer Rise, Leg 56. In: Scientific Party, Initial Reports of the Deep Sea Drilling Project, 56, 57, Pt. 1: Washington (U.S. Govt. Printing Office), 399–446. https://doi.org/10.2973/dsdp.proc.5657.107.1980
Strasser M, Kolling M, dos Santos FC, Fink HG, Fujiwara T, Henkel S, Ikehara K, Kanamatsu T, Kawamura K, Kodaira S, Romer M, Wefer G, R/V Sonne Cruise SO2019A and JAMSTEC Cruise MR12-E01 scientists (2013) A slump in the trench: tracking the impact of the 2011 Tohoku-Oki earthquake. Geology 41:935–938. https://doi.org/10.1130/G34477.1
Takahashi N, Kodaira S, Tsuru T, Park JO, Kaneda Y, Suyehiro K, Kinoshita H, Abe S, Nishino M, Hino R (2004) Seismic structure and seismogenesis off Sanriku region, northeastern Japan. Geophys J Int 159:129–145. https://doi.org/10.1111/j.1365-246X.2004.02350.x
Tanioka Y, Satake K (1996) Fault parameters of the 1896 Sanriku tsunami earthquake estimated from tsunami numerical modeling. Geophys Res Lett 23(13):1549–1552. https://doi.org/10.1029/96GL01479
Todd EK, Schwartz SY (2016) Tectonic tremor along the northern Hikurangi Margin, New Zealand, between 2010 and 2015. J Geophys Res 121(12):8706–8719. https://doi.org/10.1002/2016JB013480
Tsuru T, Park JO, Takahashi N, Kodaira S, Kido Y, Kaneda Y, Kono Y (2000) Tectonic features of the Japan Trench convergent margin off Sanriku, northeastern Japan, revealed by multichannel seismic reflection data. J Geophys Res 105:16403–16413. https://doi.org/10.1029/2000JB900132
Tsuru T, Park JO, Miura S, Kodaira S, Kido Y, Hayashi T (2002) Along-arc structural variation of the plate boundary at the Japan Trench margin: implication of interpolate coupling. J Geophys Res 107:2357. https://doi.org/10.1029/2001JB001664
Uchida N, Kirby SH, Umino N, Hino R, Kazakami T (2016) The great 1933 Sanriku-oki earthquake: reappraisal of the main shock and its aftershocks and implications for its tsunami using regional tsunami and seismic data. Geophys J Int 206:1619–1633. https://doi.org/10.1093/gji/ggw234
Ujiie K, Tanaka H, Saito T, Tsutsumi A, Mori JJ, Kameda J, Brodsky EE, Chester FM, Eguchi N, Toczko S, Expedition 343 and 343T Scientists (2013) Low coseismic shear stress on the Tohoku-Oki megathrust determined from laboratory experiments. Science 342:1211–1214. https://doi.org/10.1126/science.1243485
Von Huene R, Culotta R (1989) Tectonic erosion at the front of the Japan Trench convergent margin. Tectonophysics 160:75–90
Wessel P, Luis JF, Uieda L, Scharroo R, Wobbe F, Smith WHF, Tian D (2019) The generic mapping tools version 6. Geochem Geophys Geosyst 20:5556–5564. https://doi.org/10.1029/2019GC008515
Zhao D, Huang Z, Umino N, Hasegawa A, Kanamori H (2011) Structural heterogeneity in the megathrust zone and mechanism of the 2011 Tohokuoki earthquake (Mw 9.0). Geophys Res Lett 38(17):L17308. https://doi.org/10.1029/2011GL048408

Publisher's Note